Chemical Engineering Journal 165 (2010) 240–249

Contents lists available at ScienceDirect

Chemical Engineering Journal

journal homepage: www.elsevier.com/locate/cej

Simple method for preparation of chitosan/poly(acrylic acid) blending hydrogel beads and adsorption of copper(II) from aqueous solutions☆

Jie Dai[a], Han Yan[a], Hu Yang[a,*], Rongshi Cheng[a,b]

[a] Key Laboratory of Mesoscopic Chemistry of MOE, Department of Polymer Science and Technology, School of Chemistry and Chemical Engineering, Nanjing University, Nanjing 210093, PR China
[b] College of Material Science and Engineering, South China University of Technology, Guangzhou 510641, PR China

ARTICLE INFO

Article history:
Received 24 July 2010
Received in revised form
18 September 2010
Accepted 20 September 2010

Keywords:
CS/PAA-GLA beads
CS-GLA beads
Adsorption of copper(II)
Adsorption mechanisms

ABSTRACT

In this paper, poly(acrylic acid) blended chitosan (CS/PAA) hydrogel beads have been prepared by one-step method simply. It was found that glutaraldehyde (GLA) cross-linked CS/PAA beads had better stability in lower pH solutions and higher mechanical strength than CS-GLA beads without PAA. Results from removal of Copper(Cu) ions from aqueous solutions showed that the adsorption capacity of CS/PAA-GLA beads was greater than that of CS-GLA beads. Moreover, the adsorption capacity for two types of beads both showed temperature independent. Furthermore, the adsorption isotherms of various beads at different temperatures were both better fitted for Langmuir equation, while the adsorption kinetics was both better described by the pseudo-second order equation. Furthermore, Fourier transform infrared spectroscopy and X-ray photoelectron spectroscopy have been employed to investigate the adsorption mechanisms from molecular levels. It indicated that the efficient effects of CS/PAA-GLA beads on removal of Cu(II) resulted from the fact that carboxyl groups were facile to form bidentate carboxylates with metal ions. In addition, Cu(II) ions could be desorbed efficiently from both aforementioned beads at pH below 4.0, and the adsorption capacity of the regenerated beads had no loss until six cycles.

1. Introduction

Over the years, with rapid development of modern industries, the problem of water pollution turns more serious day by day. In the view of the characteristics of current water pollution, the heavy metal contamination increases rapidly in water resources, and has drawn more and more attentions because of the toxic effect on the human beings, animals and plants in the environment [1–3]. Among those metal pollutions, evidences show that copper may be a human carcinogen and can cause harm to the aqueous fauna, although copper is very important for the human beings as an essential trace element. The criterion of Cu(II) in drinking water is 2.0 mg/L established by World Health Organization. The potential sources of copper(II) in industrial effluents include metal cleaning and plating baths, pulp, and paper board mills, wood pulp production, and the fertilizer industry, etc. [4,5].

Conventional methods including chemical precipitation, filtration, electrochemical treatment, and ion exchange have been adopted for removal of heavy metal ions from wastewaters. Most of these methods are expensive and incapable of removing trace levels of heavy metal ions [6–8]. Thus, adsorption, especially biosorption, as an effective and economical method has become an alternative technique for removal of heavy metal from diluted solutions.

In the latest years, many biological materials have been employed as adsorbents to remove heavy metals from wastewaters [9,10]. Particularly, chitosan(CS) being a kind of very important environment-friendly materials, also named poly(β-1-4)-2-amino-2-deoxy-D-glucopyranose, is produced through the deacetylation of chitin, which is the second most abundant natural polymers in the world [11–14]. Furthermore, chitosan, as a kind of efficient adsorbents, still bears excellent chelating effect for the abundant free –OH and $-NH_2$ groups, and could carry out effectively removal of metal ions, humic acids and synthetical surfactants at low concentrations. Therefore, it is believed that chitosan is very useful and powerful in the field of wastewater treatment [15–17].

In order to improve the adsorption capacity, hydrogel beads has been made instead of flakes or powder chitosan because the gel formation in producing chitosan hydrogel beads decreases the crystallinity of the flakes or powder adsorbent [10,18]. Furthermore, chemical cross-linking is necessarily applied to prevent the dissolution of chitosan beads in acidic media, although the adsorption capacity of cross-linked chitosan beads is reduced, especially at low pH solution, because of consumption of the amine groups in chitosan during the cross-linking reaction [19,20]. Some of the most

☆ Supported by the Key Natural Science Foundation of China (grant no. 50633030 and 51073077).
* Corresponding author. Tel.: +86 25 83686350; fax: +86 25 83317761.
E-mail address: yanghu@nju.edu.cn (H. Yang).

1385-8947/$ – see front matter © 2010 Elsevier B.V. All rights reserved.
doi:10.1016/j.cej.2010.09.024

commonly used cross-linking agents are glutaraldehyde (GLA), epichlorohydrine (ECH) and ethylene glycol diglycidyl ether (EGDE) [20,21].

In addition, chemical modifications have also been applied to prepare various chitosan-based beads, including grafting of a new functional group and polymer blending [10,17,18,22–24]. As is known, carboxyl groups have great chelating effects with many heavy metal ions. Therefore, various carboxylated chitosan products have been reported [22,23,25–27]. Therein, poly(acrylic acid) (PAA) is a type of water soluble polymers, containing a carboxyl group in each repeated unit and shows anionic polyelectrolyte features, which provide favorable or attractive electrostatic interaction for adsorption of metal ions [28]. Bai et al. [22] prepared PAA surface-functionalized chitosan beads, and found that the adsorption of lead ions has been highly enhanced. Wang et al. [27] reported a composites of PAA grafted chitosan with attapulgite for fast removal of copper(II) ions from aqueous solutions.

In this work, a simple method only one step for preparation of CS/PAA blending hydrogel beads by coprecipitation of the mixed solutions of chitosan and PAA in sodium hydrate aqueous solutions has been provided, which method suits for preparation of PAA modified chitosan adsorbents in large-scale. In addition, the mechanical properties of the hydrogel beads have been investigated also, which is significant in real applications. On the other hand, the adsorptions of Cu(II) ions onto CS/PAA-GLA and CS–GLA beads from aqueous solutions have been studied, respectively, including the effects of the initial pH value of Cu(II) solution and temperature. Furthermore, the isothermal adsorption equilibrium, kinetics, desorption and reusability were also included in this study. Meanwhile, Fourier transform infrared spectroscopy, and X-ray photoelectron spectroscopy were performed for studying the adsorption mechanisms from molecular levels further.

2. Experimental

2.1. Materials

Chitosan, which degree of deacetylation was 90.5% and viscosity average molecular weight was 3.0×10^5 g/mol, was purchased from Shandong Aokang Biological Co. Ltd., China. Poly(acrylic acid) (PAA) was prepared by radical polymerization using toluene as solvent in lab, and viscosity average molecular weight of PAA was 1.0×10^5 g/mol. Glutaraldehyde (GLA) solution (25%, w/w) was supplied by Sinopharm Chemical Reagent Co. Ltd., China. $CuSO_4 \cdot 5H_2O$, hydrochloric acid (HCl), sodium hydrate (NaOH) and other reagents used in this work were all A.R. grade reagents. Distilled water was used in all experiments.

2.2. Preparation of various CS beads

2.2.1. CS-GLA beads

The desired amount of chitosan powders was dissolved in 200 ml 0.5% (w/w) HCl aqueous solution. The viscous solution was left overnight for mixing homogenously before adding dropwise into 3.0 mol/L NaOH alcohol–water solution (1/2, v/v) to prepare chitosan beads. Then, the chitosan beads were filtered, rinsed with distilled water until the solution pH became the same as that of the fresh distilled water. At last, chitosan beads were suspended into GLA solutions, and left standing for 3.5 h at room temperature under continuous stirring. Finally, the CS-GLA beads were washed with distilled water until pH reached to neutral. The beads were stored in distilled water for further application. Based on the formulations as listed in Table 1, various CS-GLA beads have been prepared.

2.2.2. CS/PAA-GLA beads

The HCl aqueous solution of chitosan has been prepared the same as before. The desired amount of PAA powders was dissolved in distilled water for further preparation. The solute mass ratio of CS to PAA is 2:1. Then, the PAA solution was mixed with the chitosan solution, and the blended hydrogel has been formed immediately for the strong electrostatic interaction between the amine groups of chitosan and the carboxyl groups of PAA. The 36% (w/w) HCl solution was added dropwise into the gel until it became homogenous and clear solution again. By the same method as before, the viscous solution was added dropwise into NaOH solution to form CS/PAA blending hydrogel beads. After washed to neutral by distilled water, the CS/PAA beads were chemical cross-linked by GLA for 3.5 h at room temperature. Finally, the CS/PAA-GLA beads were washed to neutral, and stored in distilled water for further application. Based on the formulations as listed in Table 1, various CS/PAA-GLA beads have been prepared also.

2.3. Dissolution experiment

The stability of CS-GLA and CS/PAA-GLA beads has been tested by the dissolution experiment. Various beads were put in 0.3 mol/L HCl aqueous solutions, then distilled water for test, respectively.

2.4. Hydration rate test

Hydration rate (*HR*) is applied to describe the content of water in the hydrogel beads. *HR* was calculated according to the following equation:

$$HR(\%) = \frac{W_h - W_d}{W_h} \times 100 \quad (1)$$

where W_h and W_d are the weight of the hydrated and dried beads, respectively. The hydrated CS-GLA and CS/PAA-GLA beads were dried in a vacuum desiccator at room temperature until the weight kept constant.

2.5. Scanning electron microscope (SEM)

After being sputter coated with gold, the surface morphologies of these dried beads were observed directly with a scanning electron microscope (Type SSX-550; Shimadzu Co., Japan). The electron micrographs were taken with an acceleration voltage of 25.0 kV.

Table 1
Hydration rate, solubility, stability effect and mechanical property of various CS-GLA and CS/PAA-GLA beads.

Beads	GLA concentration (mol/L)	Hydration rate (%)	Solubility and stability effects		Mechanical property
		Distilled water	0.3 M HCl	Distilled water after 0.3 M HCl	Burst strength (mN)
CS0	0	94.07	Soluble	–	315.01
CS1	0.0313	93.76	Insoluble	Broken	390.78
CS2	0.0938	92.74	Insoluble	Stable	519.52
CS/PAA1	0.0313	93.08	Insoluble	Stable	623.43
CS/PAA2	0.0938	92.02	Insoluble	Stable	676.36

2.6. Fourier transform infrared spectroscopy (FTIR)

The Fourier transform infrared spectra of CS-GLA and CS/PAA-GLA beads before and after adsorption of copper(II) ions were recorded using Fourier transform infrared spectrometer (Type TENSOR 27; Bruker Co.; Germany). All samples were prepared as potassium bromide tablets, and the interval of tested wave numbers was 500–4000 cm^{-1}.

2.7. Mechanical property

Burst strength of various beads was tested by Texture Analyser (Type TA. XTplus; SMS Co.; UK), respectively, and the P36R Cylinder Probes has been employed. Five specimens were tested for each sample.

2.8. X-ray photoelectron spectroscopy (XPS)

X-ray photoelectron spectroscopy of CS-GLA and CS/PAA-GLA beads before and after adsorption of Cu(II) ions were recorded by an X-ray photoelectron spectrometer (Type K-Alpha; Thermo Scientific Corp., America) with an Al Kα X-ray source.

2.9. Adsorption experiments

2.9.1. Adsorption of copper(II) at different initial pH

The influences of different initial pH to adsorption of copper(II) onto CS-GLA and CS/PAA-GLA beads were studied, respectively. The range of initial pH values was 1.0–5.0, adjusted by 0.1 mol/L HCl, and the initial concentration of Cu(II) aqueous solution was 385.0 mg/L. Various beads were weighed and immerged into Cu(II) solutions with different pH values under continuous stirring at room temperature for 24 h. The initial and final Cu(II) concentrations of solutions were analyzed with ethylenediamine as developing agent at a wavelength of 546 nm by vis spectrophotometer (Type 7200; Unico Corp.; China). The amount of adsorption, q (mg/g), was calculated according to the following equation:

$$q = \frac{(C_0 - C_e)V}{m} \quad (2)$$

where C_0 (mg/L) and C_e (mg/L) are the initial and final Cu(II) concentrations of the solution, V (L) is the volume of the copper(II) solution, and m (g) is the dried weight of the CS-GLA and CS/PAA-GLA beads, respectively.

2.9.2. Adsorption equilibrium study

CS2 and CS/PAA1 beads, nominated in Table 1, have been selected for further adsorption equilibrium and kinetics study. The experiments were conducted at different temperatures: 10, 21, 30, and 40 °C, respectively. The concentrations of Cu(II) solutions are ranging from 40 to 450 mg/L. CS-GLA and CS/PAA-GLA beads were weighed and immerged in Cu(II) solutions with various concentrations and temperatures under continuous stirring at initial pH 5.0 for 24 h. The same analysis method as mentioned before has been employed to detect the initial and final Cu(II) concentrations of solutions by vis spectrophotometer. The amount of adsorption was calculated based on Eq. (2).

2.9.3. Kinetic adsorption experiments

The kinetic adsorption experiments were also measured at varied temperatures: 10, 21, 30, and 40 °C, respectively. The initial concentration of Cu(II) solutions and the pH value were fixed at 385.0 mg/L and 5.0, respectively. Various beads were weighed and immerged into Cu(II) solutions under continuous stirring at varied temperatures. Then, 1 mL of sample solutions were taken out at desired time intervals to analyze the current Cu(II) concentration, meanwhile, the same volume of water with pH 5.0 was added into the bulk solutions to keep the volume constant. The adsorption of Cu(II) at time t_i, $q(t_i)$ (mg/g), was calculated from the following equation:

$$q(t_i) = \frac{(C_0 - C_{t_i})V_o - \sum_2^{i-1} C_{t_{i-1}} V}{m} \quad (3)$$

where C_0 and C_{t_i} (mg/L) are the initial Cu(II) concentration and Cu(II) concentrations at time t_i, respectively. V_0 and V_s (L) are the volume of the Cu(II) solution and that of the sample solution taken out every time for Cu(II) concentration analysis, respectively. Here, V_s is equal to 0.001 L. And m (g) is the dried weight of the beads.

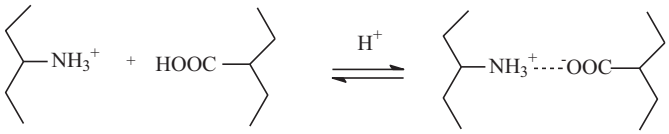

Scheme 1. The invert process of the electrostatic interaction between the amine groups of chitosan and the carboxyl groups of PAA.

2.10. Desorption and reusability experiments

2.10.1. Desorption experiment

The effects of different initial pH on desorption of Cu(II) from CS-GLA and CS/PAA-GLA beads were studied at room temperature, respectively. Various beads saturated with Cu(II) were weighed, and then immerged into different aqueous solutions with different pH values ranged from 1.0 to 12.0 under continuous stirring at room temperature for 24 h. The final Cu(II) concentrations in solution were analyzed based on aforementioned method to estimate the amount of desorption.

2.10.2. Recycling experiments

The various Cu(II) loaded beads were recovered from 0.1 mol/L HCl solution, and then collected from the solutions by filtration, washed with distilled water, and then reused in the next cycle of adsorption experiments. The adsorption–desorption experiments were conducted for six cycles. All the experiments were performed at room temperature.

3. Results and discussion

3.1. Preparation of CS-GLA and CS/PAA-GLA beads

The CS-GLA beads have been prepared according to reported method [13,18], and the detailed preparation processes for CS/PAA-GLA beads were described in the experimental part. At the beginning, after mixing the chitosan and PAA solutions, the complex hydrogel has formed immediately for the strong electrostatic interaction between amine and carboxyl groups. Then, a high concentrated HCl aqueous solution was added into the mixture dropwise until the gel dissolved to homogenous and clear solution, because the original strong electrostatic interactions could be broken by protonation of amine and carboxyl groups. The invert process was described in Scheme 1. Finally, the CS/PAA blending beads have been gotten by coprecipition of their mixed solutions in sodium hydrate solutions as usual. For guarantee the stability in acidic media, CS/PAA beads have been also chemically cross-linked by GLA further.

The macro- and micro-images of aforementioned two kinds of beads were shown in Supporting Information Fig. S1 and S2, respectively. It was found that the appearance of CS/PAA-GLA beads was spherical and primrose yellow color, and the average diameter was

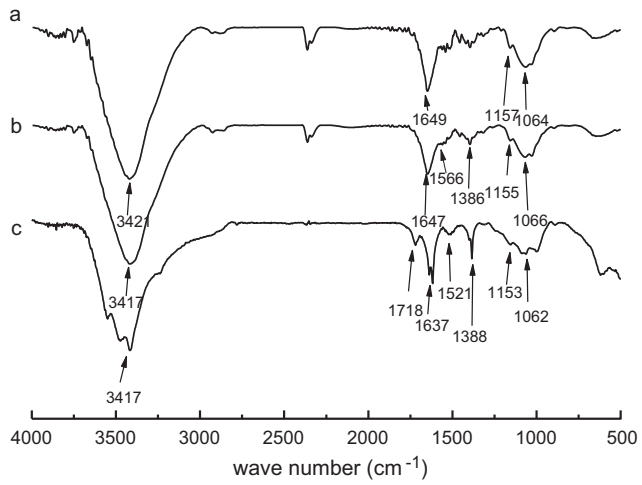

Fig. 1. FTIR spectra of CS-GLA (a), Na-form CS/PAA-GLA (b), and H-form CS/PAA-GLA (c) hydrogel beads.

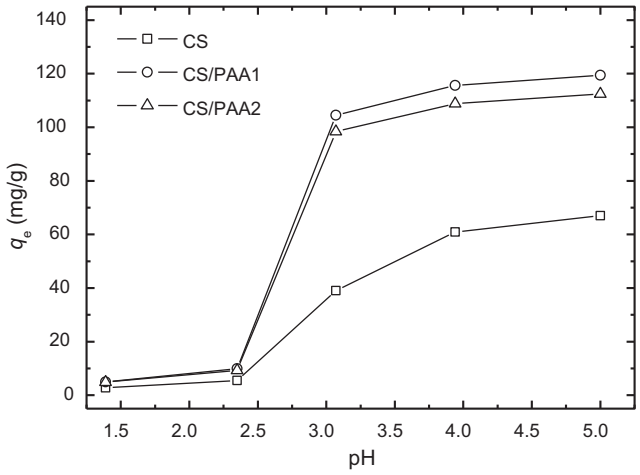

Fig. 2. Effect of initial solution pH values on adsorption capacities of Cu(II) on CS-GLA and CS/PAA-GLA beads (initial concentration of Cu(II) in the solution was 385.0 mg/L).

near 2.5 mm, which was similar to that of CS-GLA beads, but surface was denser for formation of CS/PAA complex.

For further characterization, FTIR spectra of CS-GLA and CS/PAA-GLA beads were obtained, and shown in Fig. 1. The characteristic peaks of CS-GLA in Fig. 1a were located around as follows: the overlapped peaks around 3421 cm^{-1} corresponded to –OH and –NH stretching vibrations, 1649 cm^{-1} was due to –NH bending vibration in $–NH_2$, 1157 cm^{-1} was assigned to –CN stretching vibration, and 1064 cm^{-1} was corresponded to –C–O stretching vibration in –C–OH, respectively. As for CS/PAA-GLA beads, since they were obtained from coprecipitation in sodium hydrate solution, the carboxyl groups were deprotonized and formed Na-form beads even washed to neutral. For comparison, the blending beads were treated in acidic solution to be H-form ones before FTIR measurement. The FTIR spectra of Na-form and H-form CS/PAA-GLA beads were shown in Fig. 1b and c, respectively. The arm peak around 1566 cm^{-1} and the single peak at 1386 cm^{-1} were both assigned to $–COO^-$ groups in Fig. 1b. However, in the FTIR spectrum of H-form CS/PAA-GLA beads of Fig. 1c, two new characteristic peaks appeared at 1718 and 1521 cm^{-1}, which were assigned to –COOH and $–NH_3^+$, respectively. It indicated that PAA has been blended in the chitosan beads successfully.

3.2. Swelling, stability and mechanical properties

Chitosan was usually facile to dissolve in acidic media for protonation of the amine groups, but insoluble in neutral or alkaline solutions. Furthermore, CS beads were fragile, and the lower mechanical properties made it difficult to apply in practice. For improvement of the stability in low pH and mechanical properties of CS beads, GLA was applied to prepare chemical cross-linked CS beads. From Table 1, GLA cross-linked CS and CS/PAA beads could not dissolve, but be swollen in HCl aqueous solution. Hydration rate of various beads, which were all higher than 90%, indicated that CS-GLA and CS/PAA-GLA beads contained high content of water. In addition, from Table 1, hydrate rate of aforementioned two types of beads both slightly decreased with the amount of GLA increase. It was believed that the porous structures in swollen beads was increased and magnified due to high hydration rate, which was beneficial to increase the amount and rate of the adsorption.

Furthermore, based on Table 1 and Supporting Information Fig. S3, it was found that the burst strength was enhanced as the amount of cross-linking agent increased, but the swollen CS beads cross-linked with low amount of GLA was still easy to break after soaked in pure water for chitosan shrinking in its poor solvent. However, after PAA was blended into the CS beads, the stability and burst strength of CS/PAA-GLA, even using lower amount of cross-linking agent, were improved evidently in comparison to these of CS beads. It was due to the typical semi-interpenetrating polymer network (semi-IPN) structures of CS/PAA-GLA hydrogel beads, and the strong electrostatic interactions between the protonized amine groups of chitosan and the carboxyl groups of PAA, both of which increased the intension of CS beads greatly.

3.3. Effect of initial pH on adsorption of Cu(II)

The CS/PAA-GLA hydrogel beads were employed for removal of Cu(II) from aqueous solution. Fig. 2 showed the adsorption capacities of CS2, CS/PAA1 and CS/PAA2 for Cu(II) ions in solutions with initial pH varied from 1.0 to 5.0, respectively. At pH values higher than 5.0, precipitation of Cu(II) ions as $Cu(OH)_2$ occurred simultaneously, and could not lead to accurate interpretation of adsorption. In addition, the stability of CS1 beads were too low to further test based on Table 1. According to Fig. 2, it was found that the adsorption capacity of Cu(II) ions onto each adsorbent increased as the initial pH value of the solution increased. At lower pH, the adsorption capacity of CS-GLA beads were low, because the amine groups in the beads easily formed protonation which induced an electrostatic repulsion of Cu(II) ions. Therefore, competition existed between protons and Cu(II) ions for adsorption sites, which resulted in the decrease of adsorption capacity [20].

As for CS/PAA-GLA beads, in addition to amine groups, carboxyl groups had various electrostatic interactions with Cu(II) ions at different pH conditions. At higher pH, –COOH groups of CS/PAA-GLA beads were dissociated into $–COO^-$ groups. This made the electrostatic interaction between the adsorbents and Cu(II) ions become significantly favorable or attractive, and hence resulted in the increase of Cu(II) ions uptake [22]. Furthermore, the adsorption capacity for CS/PAA2 was slightly lower than that for CS/PAA1 because of consumption of more amine groups by crossing-linking agents [19,20]. However, both CS/PAA-GLA beads had shown much higher adsorption capacities than CS-GLA beads in whole measured pH range, which indicated that PAA played an important role in removal of Cu(II) ions.

Table 2
The comparison of the Langmuir, Freundlich, and Sips adsorption constants obtained from adsorption isotherms of Cu(II) ions for CS-GLA and CS/PAA-GLA beads at different temperatures at pH 5.0.

Beads	T (°C)	$Q_{m,exp}$ (mg/g)	Langmuir constants			Freundlich constants			Sips constants		
			$Q_{m,cal}$ (mg/g)	B ($\times 10^3$ L/mg)	R^2	K	n	R^2	q_m (mg/g)	$b \times 10^3$ (L/mg)	$1/n$	R^2
CS-GLA	10	66.20	78.24	17.44	0.997	7.71	2.59	0.984	112.53	6.53	0.68	0.987
	21	66.55	77.16	18.21	0.997	8.07	2.66	0.983	117.58	5.69	0.65	0.988
	30	65.97	77.94	17.63	0.997	7.71	2.59	0.984	108.47	7.28	0.70	0.988
	40	66.36	78.30	17.18	0.998	7.67	2.59	0.986	108.65	7.09	0.69	0.989
CS/PAA-GLA	10	120.01	126.42	64.01	0.998	50.84	6.64	0.951	144.94	41.19	0.69	0.963
	21	121.55	126.26	63.72	0.998	50.80	6.63	0.951	145.27	40.49	0.68	0.959
	30	119.93	126.26	64.66	0.998	50.94	6.66	0.951	144.75	41.61	0.69	0.961
	40	119.58	125.63	63.35	0.998	50.09	6.58	0.949	144.49	40.19	0.69	0.951

3.4. Isothermal adsorption equilibrium

The equilibrium isotherm was fundamental in describing the interactive behavior between the solutes and adsorbent. The adsorption isotherms for Cu(II) on CS-GLA and CS/PAA-GLA beads was presented in Supporting Information Fig. S4, respectively. From Fig. S4a and b, it was found that the adsorption isotherms for two types of beads both showed temperature independent, which illuminated that the equilibrium amount of the adsorbed Cu(II) ions could not be affected by temperature. At the beginning, adsorption capacity of Cu(II) ions increased linearly with the initial concentrations of Cu(II) increasing, then reached to surface saturation at high concentrations around 200 mg/L. It indicated that, at lower initial concentrations of Cu(II) ions, the adsorption sites on the beads were sufficient and the adsorption capacity relied on the amount of Cu(II) ions transported from the bulk solution to the surfaces of the beads. However, at higher initial concentrations of Cu(II) ions, the adsorption sites on the surfaces of the beads reached to saturation, and the adsorption of Cu(II) ions achieved equilibrium [10]. Furthermore, the equilibrium uptakes of Cu(II) on CS/PAA-GLA beads were greater than that on CS-GLA beads. Based on Supporting Information Fig. S4 and Table 2, the experimental equilibrium uptakes of Cu(II) on CS-GLA and CS/PAA-GLA beads were average 66.27, and 120.27 mg/g, respectively.

The correlation of equilibrium data using either a theoretical or empirical equation was essential for the adsorption interpretation and prediction of the extent of adsorption. The adsorption data was generally interpreted by Langmuir, Freundlich, Sips, Dubinin–Radushkevich (D–R) and Dubinin–Radushkevich–Kaganer (D–R–K) isotherm models. The Langmuir model was based on the assumption of a structurally homogeneous adsorbent where all adsorption sites were identical and energetically equivalent. The Langmuir model was represented as follows:

$$\frac{C_e}{q_e} = \frac{1}{q_{\max} b} + \frac{C_e}{q_{\max}} \tag{4}$$

where q_e is the amount of Cu(II) ions adsorbed at equilibrium (mg/g), C_e is the liquid-phase Cu(II) concentration at equilibrium (mg/L), $q_{\max}$ is the maximum adsorption capacity of the adsorbent (mg/g), and b is the Langmuir adsorption constant (L/mg), respectively.

The Freundlich model was applied to describe heterogeneous system characterized by a heterogeneity factor of $1/n$. This model described reversible adsorption and was not restricted to the formation of the monolayer. The Freundlich model was expressed as follows:

$$\log q_e = \frac{1}{n} \log(C_e) + \log K \tag{5}$$

where C_e is the liquid-phase Cu(II) concentration at equilibrium (mg/L), K is the Freundlich isotherm constant, and $1/n$ (dimensionless) is the heterogeneity factor, respectively.

Meanwhile, the Sips isotherm model could be considered as a combination of Langmuir and Freundlich equations and represented as below:

$$q_e = \frac{q_m (bC_e)^{1/n}}{1 + (bC_e)^{1/n}} \tag{6}$$

where q_m is the amount of Cu(II) ions adsorbed at equilibrium (mg/g), b is the median association constant (L/mg) and $1/n$ is the heterogeneity factor. Values for $1/n \ll 1$ indicate heterogeneous adsorbents, while values close to or even 1.0 indicate a material with relatively homogenous binding sites. In this case, the Sips model is reduced to Langmuir equation. [29]

The equilibrium data was also subjected to the D–R isotherm model for determination the nature of biosorption processes as physical or chemical process [30]. The D–R equation was given by the following relationship:

$$\ln Q_e = \ln Q_m - K\varepsilon^2 \quad (7)$$

where Q_e is the amount of the Cu(II) ions adsorbed at equilibrium, K is the constant related to the mean free energy of sorption, Q_m is the theoretical saturation capacity, and ε is the Polanyi potential ($\varepsilon = RT\ln(1 + 1/C_e)$). The D–R constant can give the valuable information regarding the mean energy of adsorption by the following equation:

$$E = (2K)^{-1/2} \quad (8)$$

In addition, D–R–K isotherm model was also applied to fit the adsorption isotherms, which was based on the assumption of a structural monolayer adsorbent by the following equation:

$$q_e = q_m \exp\left\{-\left[\frac{RT}{E_s}\ln\left(\frac{C^*}{C_e}\right)\right]^n\right\} \quad (9)$$

where q_m is the amount of Cu(II) ions adsorbed at equilibrium (mg/g), n is equal to 4, C^* is the saturation concentration. E_s is the characteristic energy of adsorption [31].

The Langmuir, Freundlich, Sips, D–R, and D–R–K model have been tried to fit the experimental data, respectively, and their parameters were listed in Table 2 and Supporting Information Table S1, respectively. The correlation coefficients (R^2) of the linear form for the Langmuir model were much closer to 1 than that of other models. Since there was no temperature dependence of adsorption capacity for the two types of beads as mentioned above, the fitted results of the Langmuir model at 30 °C were selected and shown in Supporting Information Fig. S5. It was found that the theoretic simulated curves as thin solid lines fitted the experimental data in a fairly good way, which indicated that the Langmuir model was much better to describe the adsorption of Cu(II) onto CS-GLA and CS/PAA-GLA beads than other models. This meant the monolayer coverage of Cu(II) on the surfaces of the two types of beads. Furthermore, the $Q_{m,cal}$ of CS-GLA and CS/PAA-GLA beads calculated by Langmuir model at 30 °C were 77.94, and 126.26 mg/g, respectively, both of which were close to the $Q_{m,exp}$ (65.97 and 119.93 mg/g, respectively).

In addition, Freundlich parameter, n indicated the favorability of the adsorption. If n was less than one, it indicated that adsorption intensity was good (or favorable) over the entire range of concentration studied, but if the n value was more than one, it meant that adsorption intensity was good (or favorable) at high concentration but much less at lower concentration [32]. Based on Table 2, all adsorbents showed n values more than one indicating that the adsorption intensity was favorable at high concentration.

Meanwhile, according to the analysis from Sips model in Table 2, the calculated values for $1/n$ were relatively close to 1, which indicated that these chitosan-based beads were homogeneous adsorbents.

Furthermore, according to the analysis from D–R model, the mean adsorption energy (E) could be deduced primarily. The E value of biosorption would give information about biosorption mechanisms, physical or chemical process: the adsorption behaviors could be described as the physical adsorption when E was between 1.0 and 8.0 kJ/mol, but the chemical adsorption while E was more than 8.0 kJ/mol [33]. The mean adsorption energy for Cu(II) were presented in Supporting Information Table S1, and the E values were all higher than 8.0 kJ/mol, although R^2 is less than 0.9. This indicated primarily that the adsorption behaviors for aforementioned two types of beads were both chemical adsorptions. In addition, from Supporting Information Table S1, D–R–K model showed better fitness than D–R model, which confirmed the analysis of Langmuir model further that the adsorption mechanism followed monolayer adsorption.

3.5. Adsorption kinetics

The adsorption kinetics was to establish the time course of Cu(II) uptake on the beads. It was also desirable to examine whether the adsorption behavior of Cu(II) on the beads could be described by a theoretical model that was predictive. The typical experimental results of adsorbed Cu(II) on the two types of beads versus time at different temperatures were shown in Supporting Information Fig. S6. It was found that the adsorption equilibrium time for both beads decreased as the temperature increased, which indicated that they could reach to adsorption equilibrium earlier at higher temperature.

In order to investigate the adsorption mechanisms, the pseudo-first order, pseudo-second order and intraparticle diffusion model were applied to study the experimental data. The pseudo-first order and pseudo-second order model were given as Eqs. (10) and (11), respectively [34]:

$$\log(q_e - q_t) = \log q_e - \frac{k_1}{2.303}t \quad (10)$$

$$\frac{t}{q_t} = \frac{1}{k_2 q_e^2} + \frac{t}{q_e} \quad (11)$$

where q_e and q_t are the amounts of Cu(II) ions adsorbed onto adsorbents (mg/g) at equilibrium and at time t, respectively. k_1 (min^{-1}) and k_2 ($\mathrm{g\,mg^{-1}\,min^{-1}}$) are the rate constant of first-order and second-order adsorption, respectively.

Intraparticle diffusion equation was introduced to indicate the behavior of intraparticle diffusion as the rate-limiting step in the biosorption. The intraparticle equation could be described as [35]:

$$Q_t = kpt^{0.5} + C \quad (12)$$

where Q_t is the amount of adsorbed Cu(II) ions at time t, t is the contact time (min) and k_p ($\mathrm{mg/g\,min^{0.5}}$) is the intraparticle diffusion constant.

The pseudo-first order, pseudo-second order and intraparticle diffusion model have been applied to fit the experimental data, respectively, and their parameters were all listed in Table 3. Based on the analysis of correlation coefficients (R^2), the pseudo-second order model was much better to describe the adsorption kinetics behaviors of Cu(II) ions for both beads. Furthermore, the fitted results of the pseudo-second order model at 30 °C were selected and shown in Supporting Information Fig. S7. It was found that the theoretic simulated curves as thin solid lines fitted the experimental data quite well. It indicated that the adsorption of Cu(II) ions onto various beads both followed the pseudo-second order model, and the chemisorptions were the rate controlling mechanism, whose results were fully consistent with those drawn from adsorption isotherm analysis as mentioned above. Furthermore, correlation coefficients for both pseudo-first order and intraparticle diffusion model are both higher than 0.95, which indicated that some weak interactions and intraparticle diffusion may both involve in the adsorption process.

3.6. Adsorption mechanisms

To illustrate the different adsorption capacity for Cu(II) ions by CS-GLA and CS/PAA-GLA beads from adsorption mechanisms, the FTIR spectra of two types of beads before and after adsorption of Cu(II) ions were obtained and shown in Fig. 3, respectively. In comparison with the FTIR spectra of aforementioned beads before adsorption of Cu(II) ions as shown in Fig. 3a and c, in those of beads

Table 3
Kinetic parameters for adsorption of Cu(II) onto CS-GLA and CS/PAA-GLA beads.

Beads	T(°C)	$Q_{m,exp}$ (mg/g)	First-order kinetic model			Second-order kinetic model			Intraparticle diffusion		
			$Q_{e1,cal}$ (mg/g)	k_1 (1/min)	R^2	$Q_{e2,cal}$ (mg/g)	$k_2 \times 10^4$ (mg/g min)	R^2	C	k_p (mg/g min$^{0.5}$)	R^2
CS-GLA	10	66.20	62.18	0.0396	0.996	68.12	11.95	0.998	−1.87	8.24	0.991
	21	66.55	74.89	0.0629	0.995	82.03	9.35	0.998	−0.13	10.23	0.989
	30	65.97	79.94	0.0532	0.996	80.19	14.33	0.997	−1.99	11.80	0.995
	40	66.36	83.62	0.0578	0.985	83.19	11.06	0.996	−1.78	11.89	0.992
CS/PAA-GLA	10	120.01	116.66	0.0225	0.970	160.51	2.13	0.993	15.25	10.52	0.978
	21	121.55	118.58	0.0268	0.960	149.25	2.29	0.993	3.63	11.89	0.977
	30	119.93	142.17	0.0379	0.988	162.60	2.49	0.993	3.03	14.30	0.989
	40	119.58	112.43	0.0305	0.982	156.01	3.45	0.995	8.32	14.35	0.989

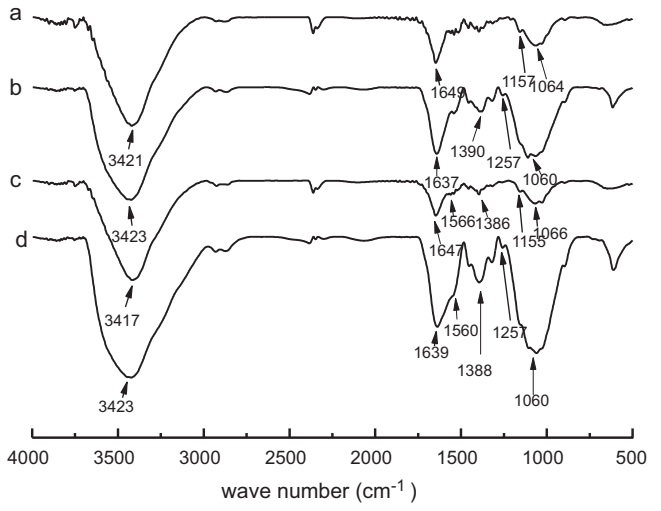

Fig. 3. FTIR spectra for the two types of beads: before (a) and after (b) adsorption of Cu(II) by CS-GLA beads, before (c) and after (d) adsorption of Cu(II) by CS/PAA-GLA beads.

after adsorption of Cu(II) ions in Fig. 3b and d, respectively, the characteristic peaks at around 1649 and 1064 cm^{-1} assigned to –NH_2 and –OH groups, respectively, both shifted to lower wave number, and the intensities of two peaks became much stronger. All these changes after adsorption of Cu(II) ions onto these beads were related to the chemical bonds involving chelating effects of –OH and –NH_2 groups with Cu(II) ions. Furthermore, in CS/PAA-GLA beads, the absorption bands at around 1560 and 1388 cm^{-1} in Fig. 3d, assigned to the symmetric and antisymmetric O–C–O stretching modes of –COO^- groups, respectively, were both enhanced and widened obviously after adsorption of Cu(II) ions, indicating that carboxyl groups were also involved in the adsorption process. In addition, the separation (Δ) between the symmetric and antisymmetric O–C–O stretching modes of the coordinated carboxylate ions in CS/PAA-GLA beads was 172 cm^{-1}. Deacon and Phillips [36] have reported that for bidentate carboxylates, the value was similar to, or less than that found in the free formate, in this case, Δ for the sodium salt was 241 cm^{-1} [37]. Thus what was observed experimentally for PAA-Cu complex has proved the existence of bidentate carboxylates, as shown in Scheme 2. It was obviously that the bidentate structures were beneficial to be adsorption of more Cu(II) ions for carboxyl groups, which might be the reason that PAA blended CS beads had higher adsorption capacity.

For further study on the complex structures, XPS has been applied, which is a useful tool for analyzing the interactions between adsorbates and adsorbents [10,17,25,26,38,39]. Fig. 4 showed the typical XPS wide scan spectra for the CS-GLA and CS/PAA-GLA beads before and after adsorption of Cu(II) ions. It was found clearly that a new peak at the binding energy (BE) of about 935.0 eV appeared after adsorption of Cu(II) ions, which was

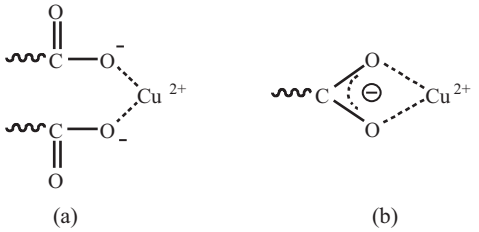

Scheme 2. The available structures of monodentate (a) and bidentate (b) carboxylates for PAA-Cu(II) complexes.

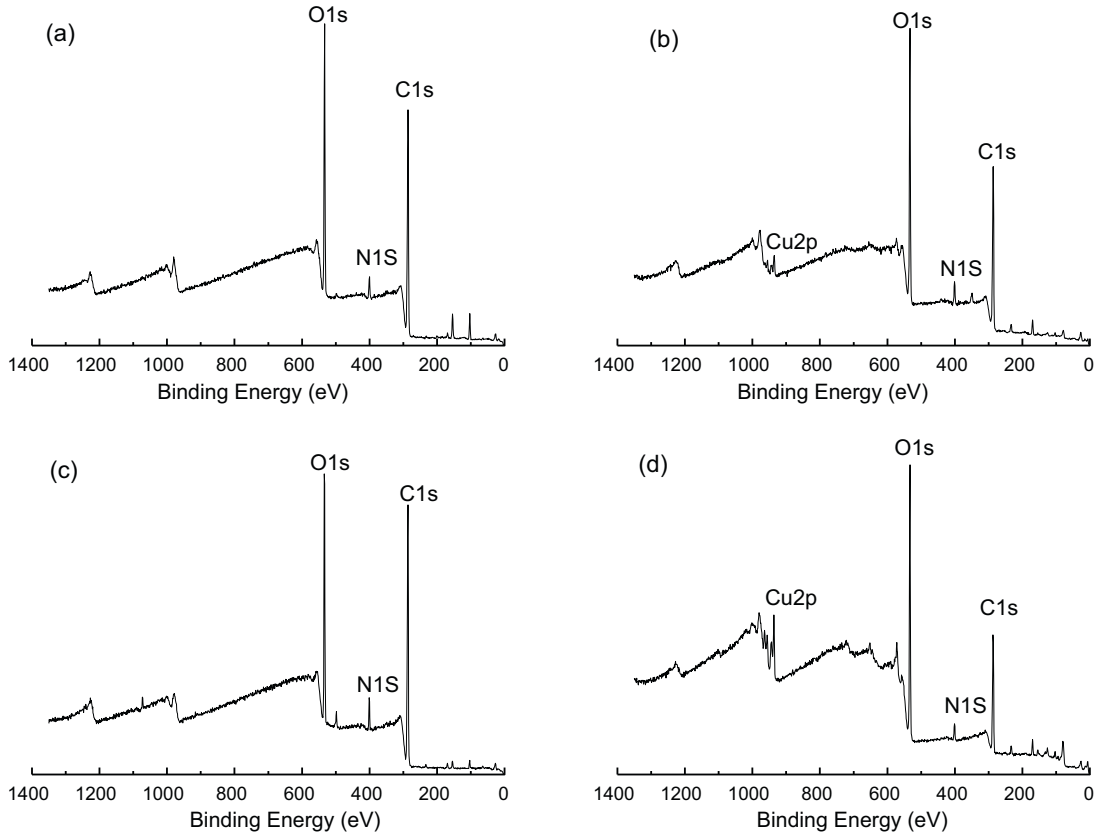

Fig. 4. The typical XPS wide scan spectra for the two types of beads: before (a) and after (b) adsorption of Cu(II) by CS-GLA beads, before (c) and after (d) adsorption of Cu(II) by CS/PAA-GLA beads.

attributed to the Cu 2*p* orbital. Therefore, the new peak provided evidence of Cu(II) being adsorbed on the surface of various beads, which were fully in agreement with the FTIR findings.

Fig. 5 showed the O 1s XPS spectra of the CS-GLA and CS/PAA-GLA beads before and after adsorption of Cu(II) ions, respectively. In Fig. 5a and b, the O 1s XPS spectra did not show significant changes of the O 1s BEs on CS-GLA beads before and after adsorption of Cu(II) ions. It was believed that the contribution of Cu-oxygen interaction to adsorption of Cu(II) ions on the CS-GLA beads was mainly through weak interaction [10].

However, as for CS/PAA-GLA beads, there were two BE peaks in O 1s spectrum before adsorption of Cu(II) ions around at 531.78 and 533.18 eV as seen in Fig. 5c, which were assigned to the oxygen atoms in the –C=O and –C–O–H groups, respectively[40]. After adsorption of Cu(II) ions, the original two BE peaks changed into one peak around 532.78 eV, which further indicated that the carboxyl groups formed bidentate carboxylates with Cu(II) as shown in Scheme 2, and the two oxygen atoms on the carboxyl group turned equivalent.

3.7. Desorption and reusability study

For practical application, desorption experiments were conducted to regenerate these Cu(II)-loaded beads. The effects of pH from 1.0 to 12.0 on desorption of Cu(II) were shown in Fig. 6. It was found that Cu(II) ions was easy to be released from both CS-GLA and CS/PAA-GLA beads at pH below 4.0, and at pH < 2.0, nearly 99% of Cu(II) ions was desorbed. However, at high pH (pH > 5.0), the Cu(II)-load beads were quite stable.

Furthermore, the adsorption and desorption processes were repeated to examine the potential of the two types of beads. Based on previous discussion, the desorption process was carried out in 0.1 mol/L HCl aqueous solution. Table 4 showed the experimental results on the amounts of Cu(II) ions adsorbed and the percentages of desorption in six consecutive adsorption–desorption cycles. It was indicated that desorption efficiency was generally high and the adsorption capacity was almost not affected. In all, due to the high recycling efficiency, these beads were qualified for practical application.

Table 4
Adsorption and desorption (recovery) behaviors of Cu(II) onto CS-GLA and CS/PAA-GLA beads.

Cycle	CS-GLA		CS/PAA-GLA	
	Adsorption amount (mg/g)	Recovery (%)	Adsorption amount (mg/g)	Recovery (%)
Cycle I	66.55	99.99	121.55	99.98
Cycle II	66.54	99.98	121.54	99.97
Cycle III	66.55	99.96	121.53	99.95
Cycle IV	66.53	99.95	121.53	99.95
Cycle V	66.53	99.94	121.52	99.94
Cycle VI	66.52	99.92	121.53	99.93

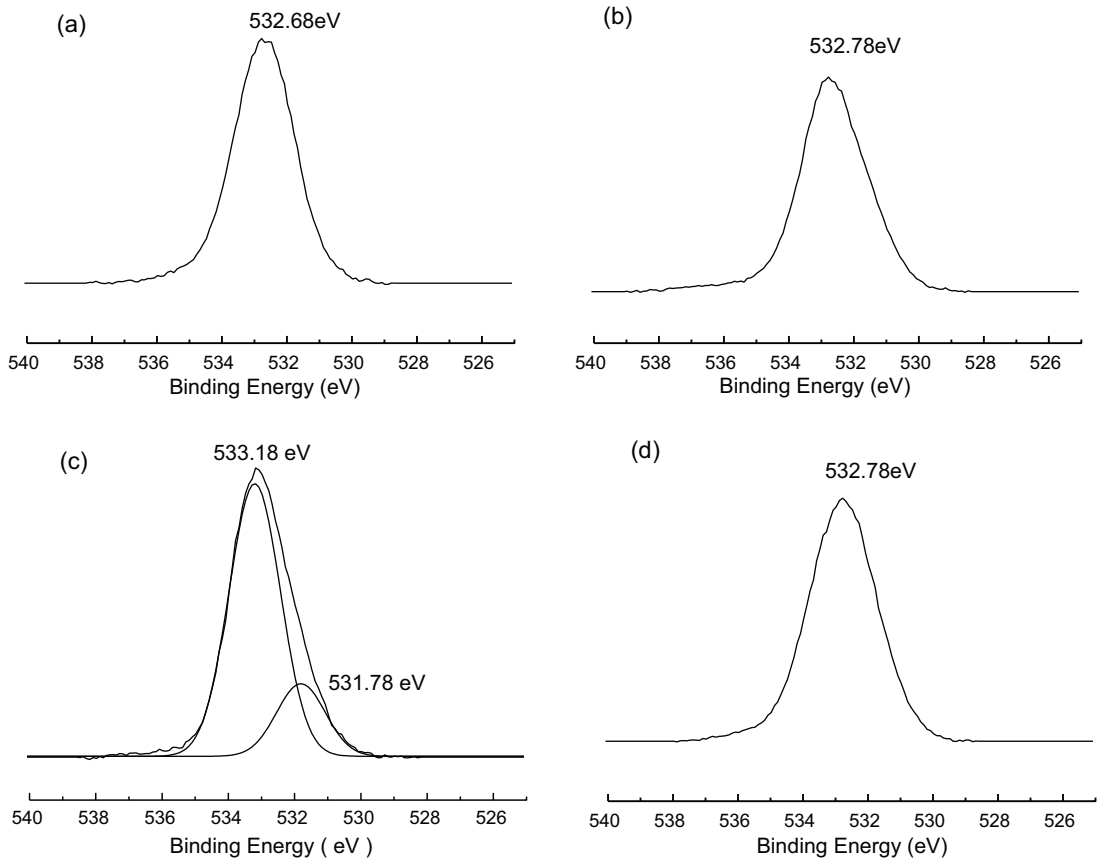

Fig. 5. The O 1s XPS spectra of the two types of beads: before (a) and after (b) adsorption of Cu(II) by CS-GLA beads, before (c) and after (d) adsorption of Cu(II) by CS/PAA-GLA beads.

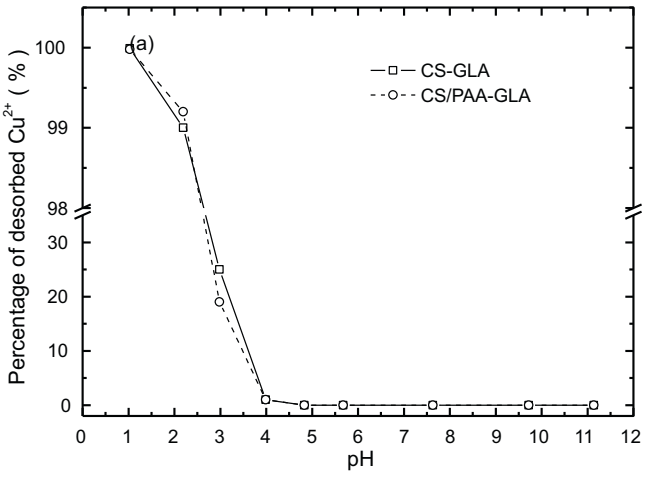

Fig. 6. Effect of pH values on Cu(II) desorption from CS-GLA and CS/PAA-GLA beads at room temperature.

4. Conclusion

CS/PAA-GLA beads have been successfully prepared by simple one-step method, and applied as an effective adsorbent for removal of Cu(II) ions from aqueous solutions. In comparison to CS-GLA beads, CS/PAA-GLA beads using a lower amount of crosslinking agent had better chemical stability in lower pH solutions and higher mechanical strength. The experimental results showed that the adsorptions of Cu(II) ions on two types of the beads were both pH dependent, but temperature independent. The adsorption capacity of Cu(II) ion on the CS beads after blending PAA was increased near one time than that on the pure CS-GLA beads. Adsorption equilibrium and kinetics study indicated that the adsorption behaviors for aforementioned two types of beads were mainly chemical monolayer adsorption. The investigation of the adsorption mechanisms from FTIR and XPS illustrated that hydroxyl and amine groups of chitosan and carboxyl groups of PAA were all involved in chelating with Cu(II) ions, and the higher adsorption capacity of CS/PAA-GLA beads was ascribed to formation of bidentate carboxylates with Cu(II) ions, which improved the efficiency for removal of metal ions. Desorption study showed that Cu(II) ions could be easily and effectively desorbed at pH below 4.0, and the regenerated adsorbent could be reused almost without any loss of adsorption capacity for a few cycles.

Appendix A. Supplementary data

Supplementary data associated with this article can be found, in the online version, at doi:10.1016/j.cej.2010.09.024.

References

[1] P.K. Rai, Heavy metal pollution in aquatic ecosystems and its phytoremediation using wetland plants: an ecosustainable approach, Int. J. Phytoremed. 10 (2008) 133–160.
[2] Y.J. An, Y.M. Kim, T.I. Kwon, S.W. Jeong, Combined effect of copper, cadmium, and lead upon Cucumis sativus growth and bioaccumulation, Sci. Total Environ. 326 (2004) 85–93.
[3] Z.L.L. He, X.E. Yang, P.J. Stoffella, Trace elements in agroecosystems and impacts on the environment, J. Trace Elem. Med. Biol. 19 (2005) 125–140.

[4] J.C.Y. Ng, W.H. Cheung, G. McKay, Equilibrium studies of the sorption of Cu(II) ions onto chitosan, J. Colloid Interface Sci. 255 (2002) 64–74.
[5] V.K. Gupta, Equilibrium uptake, sorption dynamics, process development, and column operations for the removal of copper and nickel from aqueous solution and wastewater using activated slag, a low-cost adsorbent, Ind. Eng. Chem. Res. 37 (1998) 192–202.
[6] B.S. Zhou, Technologies in industrial Wastewater Treatment, Chemical Industry Press, Beijing, 2003.
[7] N.K. Srivastava, C.B. Majumder, Novel biofiltration methods for the treatment of heavy metals from industrial wastewater, J. Hazard. Mater. 151 (2008) 1–8.
[8] A. Dabrowski, Z. Hubicki, P. Podkoscielny, E. Robens, Selective removal of the heavy metal ions from waters and industrial wastewaters by ion-exchange method, Chemosphere 56 (2004) 91–106.
[9] G. Crini, Recent developments in polysaccharide-based materials used as adsorbents in wastewater treatment, Prog. Polym. Sci. 30 (2005) 38–70.
[10] N. Li, R.B. Bai, Copper adsorption on chitosan–cellulose hydrogel beads: behaviors and mechanisms, Sep. Purif. Technol. 42 (2005) 237–247.
[11] W.S.W. Ngah, S. Fatinathan, Chitosan flakes and chitosan–GLA beads for adsorption of *p*-nitrophenol in aqueous solution, Colloids Surf. A 277 (2006) 214–222.
[12] S. Chatterjee, M. Adhya, A.K. Guha, B.P. Chatterjee, Chitosan from Mucor rouxii: production and physico-chemical characterization, Process Biochem. 40 (2005) 395–400.
[13] T.D. Jiang, Chitosan, Chemical Industry Press, Beijing, 2007.
[14] M. Rinaudo, Chitin and chitosan: properties and applications, Prog. Polym. Sci. 31 (2006) 603–632.
[15] T.Y. Hsien, G.L. Rorrer, Heterogeneous cross-linking of chitosan gel beads: kinetics, modeling, and influence on cadmium ion adsorption capacity, Ind. Eng. Chem. Res. 36 (1997) 3631–3638.
[16] R. Schmuhl, H.M. Krieg, K. Keizer, Adsorption of Cu (II) and Cr (II) ions by chitosan: kinetics and equilibrium studies, Water SA 27 (2001) 1–8.
[17] L. Jin, R.B. Bai, Mechanisms of lead adsorption on chitosan/PVA hydrogel beads, Langmuir 18 (2002) 9765–9770.
[18] W.S.W. Ngah, S. Fatinathan, Adsorption of Cu(II) ions in aqueous solution using chitosan beads, chitosan–GLA beads and chitosan–alginate beads, Chem. Eng. J. 143 (2008) 62–72.
[19] N. Li, R.B. Bai, A novel amine-shielded surface cross-linking of chitosan hydrogel beads for enhanced metal adsorption performance, Ind. Eng. Chem. Res. 44 (2005) 6692–6700.
[20] W.S.W. Ngah, C.S. Endud, R. Mayanar, Removal of copper(II) ions from aqueous solution onto chitosan and cross-linked chitosan beads, React. Funct. Polym. 50 (2002) 181–190.
[21] S.T. Lee, F.L. Mi, Y.J. Shen, S.S. Shyu, Equilibrium and kinetic studies of copper(II) ion uptake by chitosan–tripolyphosphate chelating resin, Polymer 42 (2001) 1879–1892.
[22] N. Li, R.B. Bai, Highly enhanced adsorption of lead ions on chitosan granules functionalized with Poly(acrylic acid), Ind. Eng. Chem. Res. 45 (2006) 7897–7904.
[23] S.L. Sun, L. Wang, A.Q. Wang, Adsorption properties of crosslinked carboxymethyl-chitosan resin with Pb(II) as template ions, J. Hazard. Mater. B136 (2006) 930–937.
[24] N. Li, R.B. Bai, C.K. Liu, Enhanced and selective adsorption of mercury ions on chitosan beads grafted with polyacrylamide via surface-initiated atom transfer radical polymerization, Langmuir 21 (2005) 11780–11787.
[25] L. Zhao, F. Luo, J.M. Wasikiewicz, H. Mitomo, N. Nagasawa, T. Yagi, M. Tamada, F. Yoshii, Adsorption of humic acid from aqueous solution onto irradiation-crosslinked carboxymethylchitosan, Bioresour. Technol. 99 (2008) 1911–1917.
[26] S.L. Sun, L. Wang, A.Q. Wang, Adsorption properties and mechanism of cross-linked carboxymethyl-chitosan resin with Zn(II) as template ion, React. Funct. Polym. 66 (2006) 819–826.
[27] X.H. Wang, Y. Zheng, A.Q. Wang, Fast removal of copper ions from aqueous solution by chitosan-g-poly(acrylic acid)/attapulgite composites, J. Hazard. Mater. 168 (2009) 970–977.
[28] B. Smitha, S. Sridhar, A.A. Khan, Polyelectrolyte complexes of chitosan and poly(acrylic acid) as proton exchange membranes for fuel cells, Macromolecules 37 (2004) 2233–2239.
[29] S.K. Papageorgiou, F.K. Katsaros, E.P. Kouvelos, J.W. Nolan, H.L. Deit, N.K. Kanellopoulos, Heavy metal sorption by calcium alginate beads from Laminaria digitata, J. Hazard. Mater. B 137 (2006) 1765–1772.
[30] M.M. Dubinin, E.D. Zaverina, L.V. Radushkevich, Sorption and structure of active carbons. I. Adsorption of organic vapors, Zhurnal Fizicheskoi Khimii 21 (1947) 1351–1362.
[31] P.A.M. Mourao, P.J.M. Carrott, M.M.L. Ribeiro Carrott, Application of different equations to adsorption isotherms of phenolic compounds on activated carbons prepared from cork, Carbon 44 (2006) 2422–2429.
[32] Y.S. Al-Degs, M.I. El-Barghouthi, A.A. Issa, M.A. Khraisheh, G.M. Walker, Sorption of Zn(II), Pb(II), and Co(II) using natural sorbents: equilibrium and kinetic studies, Water Res. 40 (2006) 2645–2658.
[33] G Bayramoğlu, M.Y. Arıca, Construction a hybrid biosorbent using scenedesmus quadricauda and Ca-alginate for biosorption of Cu(II), Zn(II) and Ni(II): kinetics and equilibrium studies, Bioresour. Technol. 100 (2009) 186–193.
[34] Y.S. Ho, G. McKay, Comparison of chemisorption kinetic models applied to pollutant removal on various sorbents, Trans. Inst. Chem. Eng. 76B (1998) 332–340.
[35] Y.A. Yahaya, M.M. Don, S. Bhatia, Biosorption of copper (II) onto immobilized cells of pycnoporus sanguineus from aqueous solution: equilibrium and kinetic studies, J. Hazard. Mater. 161 (2009) 189–195.
[36] G.B. Deacon, R.J. Phillips, Relationships between the carbon-oxygen stretching frequencies of carboxylato complexes and the type of carboxylate coordination, Coord. Chem. Rev. 33 (1980) 227–250.
[37] E. Spinner, Vibration-spectral studies of carboxylate ions. Part III. Sodium formate, HCO_2Na and DCO_2Na; Raman-spectral depolarisation ratios in aqueous solution, and band splitting in the solid-state infrared spectrum, J. Chem. Soc. B 9 (1967) 879–885.
[38] W.L. Yan, R.B. Bai, Adsorption of lead and humic acid on chitosan hydrogel beads, Water Res. 39 (2005) 688–698.
[39] X. Zhang, R.B. Bai, Mechanisms and kinetics of humic acid adsorption onto chitosan-coated granules, J. Colloid Interface Sci. 264 (2003) 30–38.
[40] G. Beamson, Conformation and orientation effects in the X-ray photoelectron spectra of organic polymers, J. Electron. Spectrosc. Relat. Phenom. 121 (2001) 163–181.